OFFLINE ADAPTIVE POLICY LEANING IN REAL-WORLD SEQUENTIAL RECOMMENDATION SYSTEMS

Anonymous authors
Paper under double-blind review

ABSTRACT

The training process of RL requires many trial-and-errors that are costly in real-world applications. To avoid the cost, a promising solution is to learn the policy from an offline dataset, e.g., to learn a simulator from the dataset, and train optimal policies in the simulator. By this approach, the quality of policies highly relies on the fidelity of the simulator. Unfortunately, due to the stochasticity and unsteadiness of the real-world and the unavailability of online sampling, the distortion of the simulator is inevitable. In this paper, based on the model learning technique, we propose a new paradigm to learn an RL policy from offline data in the real-world sequential recommendation system (SRS). Instead of increasing the fidelity of models for policy learning, we handle the distortion issue via learning to adapt to diverse simulators generated by the offline dataset. The adaptive policy is suitable to real-world environments where dynamics are changing and have stochasticity in the offline setting. Experiments are conducted in synthetic environments and a real-world ride-hailing platform. The results show that the method overcomes the distortion problem and produces robust recommendations in the unseen real-world.

1 INTRODUCTION

Recent studies have shown that reinforcement learning (RL) is a promising approach for real-world applications, e.g., sequential recommendation systems (SRS) (Wang et al., 2018; Zhao et al.; 2019; Cai et al., 2017), which make multiple rounds of recommendations for customers and maximize long-term recommendation performance. However, the high trial-and-error costs in the real-world obstruct further applications of RL methods (Strehl et al., 2006; Levine et al., 2018).

Offline (batch) RL is to learn policies with a static dataset collected by behavior policies without additional interactions with the environment (Levine et al., 2020; Siegel et al.; Wang et al., 2020; Kumar et al., 2019). Since it avoids costly trial-and-errors in the real environment, offline RL algorithms are promising to cost-sensitive applications (Levine et al., 2020). One scheme of offline RL is learning a simulator from the dataset. In this way, RL policies can be learned from the simulator directly. Although prior works on model-based learning have achieved significant efficiency improvements in online RL by learning dynamics models (Kaiser et al., 2020; Wang et al., 2019; Heess et al.; Luo et al., 2019), building an accurate simulator is still difficult, especially in offline RL. In particular, the offline dataset may not cover the whole state-action space, and there is no way for sampling in the real-world to recover the prediction error of the learned simulator. The learned policies tend to exploit regions where insufficient data are available, which causes the instability of policy learning (Kurutach et al., 2018; Zhang et al., 2015; Viereck et al., 2017). By overcoming the problem, recent studies in offline model-based RL (Yu et al., 2020; Kidambi et al., 2020) have made significant progress in MuJoCo environments (Todorov et al., 2012). These methods learn policies with consistency penalties to avoid exploiting regions with low confidence of model prediction.

However, in real-world applications like SRS, several realistic problems of the current offline learning methods are ignored. First, take SRS as an example, customer behaviors (i.e., the environment) are non-stationary and thus change across different periods and locations. Therefore, besides the prediction error induced by model approximation, the transition in the offline dataset is also inaccurate (Krueger et al., 2019). Second, different from traditional RL environments which are overall deterministic (Brockman et al., 2016), real-world environments often introduce stochasticity. For example, after recommending a production to a customer, it is hard to model the user's decisions

without stochasticity (e.g., buying it or not), even with large enough data. Hidden confounder factors (Shang et al., 2019) obstruct the deterministic predictions. As a result, the high-confidence regions are drastically reduced and thus the exploration of policy learning are obscured.

In this paper, instead of constraining policy exploration in high-confidence regions, we study to handle the offline issue by learning to adapt. We propose an adaptive policy which is trained to make optimal actions efficiently in regions with high confidence for model prediction. While in regions with inconsistency, the policy is trained to identify the representation of each dynamics model and adapt the optimal decisions on the representation. When deploying the policy in the environment, the policy identifies the dynamics in the real-world through interaction, then adapt its behavior. The module to represent the dynamics models is named environment-context extractor. The extractor and adaptive policy should be learned in a diverse simulator set and thus can generalize to unknown situations. As a solution, we propose to use model-learning techniques with augmentation approaches to generate a simulator set to cover real-world situations. In this way, with a sufficiently large simulator set, the learned policy can adapt robustly in unknown real-world environments.

To learn the adaptive policy and environment-context extractor, we first analyze and formulate the environment context representation problem in SRS. In SRS scenarios, the environments include a two-level structure: a recommendation platform serves customers from multiple domains (e.g., in different cities and countries). For each domain, there are numerous customers with different behaviors, and the behaviors are dependent on the domain they belong to. Although there have been recent interests in learning the representation of environment parameters based on the agent's trajectories in the robotics domain (Peng et al., 2018; Akkaya et al., 2019; Zhu et al., 2018; Sadeghi et al.), the environment-context representation problem in SRS has never been proposed and a special environment structure makes the environment context agnostic based on a single customer's trajectory. As a solution, we use a special network to embed the domain information and show that the additional domain information is necessary for representing the environment contexts in SRS.

As the result, we propose Offline learning with Adaptive Policy in sequential Recommendation Systems (OapRS), as a new paradigm to solve an offline problem that policies can applied to real-world applications without any additional online sample. By learning to adapt with the representation of dynamics, OapRS is suitable to real-world scenarios in which environments are non-stationary and have stochasticity. As far as we know, this is also the first study on reality-gap and the environment-context representation problem in SRS. We conduct experiments in a reproducible synthetic environment and a real-world recommendation scenario: the driver program recommendation system of a ride-hailing platform. Our empirical evaluations demonstrate that OapRS can learn reasonable environment contexts and makes robust recommendations in unseen environments.

2 Related Work

Reinforcement learning (RL) has shown to be a promising approach for real-world sequential recommendation systems (SRS) (Wang et al., 2018; Zhao et al.; 2019; Cai et al., 2017) to make optimal recommendations with long-term performance. However, numerous online trial-and-errors in RL training are costly and thus obstruct the further applications of RL in the real-world. Many studies propose to overcome the problem by offline (batch) RL (Lange et al., 2012).

Most prior works on offline RL introduce model-free algorithms. To overcome the extrapolation error, which is introduced by the mismatch between the offline dataset and true state-action occupancy (Wang et al., 2020), these methods are designed to constrain the target policy to be close to the behavior policies (Wang et al., 2020; Kumar et al., 2019; Wu et al., 2019), apply ensemble methods for robust value function estimation (Agarwal et al., 2020), or re-weight with importance sampling (Liu et al., 2019). Most recent studies have shown that learning robust policies from the approximation of dynamics models has the potential to take actions outside the distribution on behavior policies and thus can converge to better policies (Kidambi et al., 2020; Yu et al., 2020). In particular, Kidambi et al. (2020) constructs terminating states based on a hard threshold on uncertainty, while Yu et al. (2020) uses a soft reward penalty to incorporate uncertainty. However, in stochastic and non-stationary environments, the learned dynamics have high uncertainty and thus constrain the policy to exploration in a small region.

An alternative to learning from dynamics model and deploying in real-world environments is domain randomization techniques, which is a popular solution in the robotic domain (Tobin et al., 2017; Sadeghi & Levine, 2017; Tobin et al., 2018; James et al., 2019; Peng et al., 2018; Akkaya et al.,

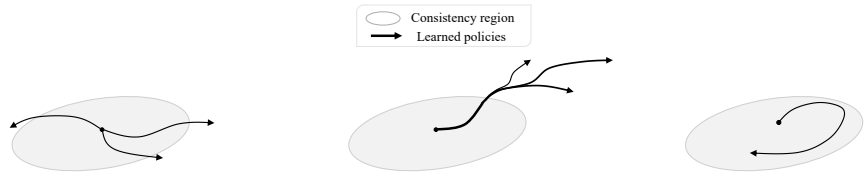

(a) domain randomization (b) OapRS (c) consistency region penalty

Figure 1: Illustration of the OapRS compared with other methods. The line denotes the optimal trajectory of the learned policies. There are several policies in domain randomization and OapRS since the methods learn to adapt in several simulators. The gray oval denotes the consistency region.

2019; Nagabandi et al.). In general, the framework trains a policy in numerous simulators, and then deploys it to unknown target domains directly. The numerous simulators are constructed by sampling different environment parameters, which are modeled by human experts with laws of physics in the real-world. The algorithms can train a uniform policy (Tobin et al., 2017; Sadeghi & Levine, 2017; Tobin et al., 2018; James et al., 2019) to maximize the expectation of the performance metrics of the simulators, or train an adaptive policy with online system identification (OSI) techniques (Peng et al., 2018; Akkaya et al., 2019; Yu et al.) to extract the representation of the dynamics of the simulators and maximize the performance metric of each simulator. In this paper, we adopt a similar idea of OSI to construct the environment-parameter extractor and the adaptive policy. However, in the offline setting, generating a simulator set by random sampling directly from the parameter space is not only hard since we do not have the exact knowledge of a representation of environment parameters to build the simulator, but inefficient because we only have access to the offline dataset to estimate the real-world dynamics.

The difference between the aforementioned methods and OapRS is shown in Figure 2. Compared with previous methods learned by uncertainty penalty (Kidambi et al., 2020; Yu et al., 2020) to reach suboptimal policies (in Figure 1(c)), we learn to make optimal decisions for all possible transitions in the states out of the consistency region (in Figure 1(b)). While learning in the entire dynamics space is an ideal solution to learn a robust policy (in Figure 1(a)), for less training cost and better efficiency, the dynamics set is generated by an offline dataset and model-learning algorithms with ensemble methods. In this way, we construct a consistency region implicitly in which optimal trajectories are similar for each simulator, while the domain randomization learns to adapt in the whole space without considering the knowledge of the offline dataset.

3 Background and Notations

In the standard RL framework, an agent interacts with an environment described as a Markov Decision Process (MDP) (Sutton & Barto, 2018). The agent learns a policy $\pi(a_t|s_t)$, which chooses an action $a_t \in \mathcal{A}$ conditional on a particular state $s_t \in \mathcal{S}$, at each time-step $t \in \{0, 1, ..., T\}$. $\mathcal{S}$ and $\mathcal{A}$ denote the state and action spaces, respectively. The reward function $r_t = r(s_t, a_t) \in \mathcal{R}$ evaluates the immediate performance of action a_t given state s_t. The goal of RL is to find an optimal policy π^*, which maximizes the multi-step cumulative discounted reward (i.e., long-term performance). The objective is to maximize $J_\rho(\pi) = \max_\pi \mathbb{E}_{\tau\sim p(\tau|\pi,\rho)} \left[\sum_{k=0}^{T} \gamma^k r_{t+k}\right]$, where γ denotes the discount factor. $p(\tau|\pi, \rho)$ is the probability of generating a trajectory $\tau := [s_0, a_0, ..., a_{T-1}, s_T]$ under the policy π and a transition dynamics $\rho(s_{t+1}|s_t, a_t)$, where T denotes the trajectory length. In particular, $p(\tau \mid \pi) := \rho_0(s_0) \prod_{t=0}^{T} \rho(s_{t+1} \mid s_t, a_t)\pi(s_t, a_t)$, where $\rho_0(s_0)$ is the initial state distribution. A common way to find an optimal policy π^* is by optimizing the policy parameters with gradient ascent along $\nabla J_\rho(\pi)$. SRS problem can be naturally formulated as an MDP. In general, the recommendation system is a policy π, while the environment consists of numerous human customers. During the learning process, the policy interacts with customers to execute the recommended action a_t based on the customer state s_t.

In the offline RL problem, we assume that we are only given a static dataset $\mathcal{D} = \{(s_i, a_i)\}_{i=1}^{N}$ collected by some unknown policies. The reward function r is given by human experts. The goal is to output a sub-optimal policy π^* to maximize J_ρ with the static dataset.

4 OapRS: Offline Learning with Adaptive Policy in Sequential Recommendation System

In the offline setting, the learned policies tend to exploit regions where the model is distorted since insufficient data are available Kurutach et al. (2018). Prior offline model-based techniques have shown great potential in learning a better policy without strict constraints in action selections (Yu et al., 2020; Kidambi et al., 2020). However, the robust offline policy learning in real-world applications is still challenging for following reasons: 1) In real-world applications like SRS, environments are non-stationary, thus, besides model learning error, the transition information of the dataset can be distorted too; 2) It is hard to predict the future states with high determinacy since there are many hidden confounders in SRS (Shang et al., 2019). Since the environment has stochasticity, learning by consistency penalties will obstruct the policy into a small region for exploration.

To output a robust policy in stochastic environments, we first study to handle the distortion problem without relying on the consistency penalty and propose the learn to adapt framwork (in section 4.1). Then we formulate and analyze the environment-context representation problem in SRS and propose an environment-context extractor and an adaptive policy optimization method (in section 4.2). Finally, we discuss important practical details to improve the robustness of simulators and policy in offline dataset (in section 4.3).

4.1 Offline adaptive policy learning

In this work, we assume that given a specific reward function r, any dynamics of environment $\rho(s'|s,a) \in \mathcal{T}$ can be fully characterized with an environment-context vector $z \in \mathcal{Z}$ (e.g., the friction coefficient in robotics), where $\mathcal{T}$ denotes a set of dynamics and $\mathcal{Z}$ denotes the space of the context vectors. Formally, there is a mapping function $\phi : \mathcal{T} \to \mathcal{Z}$. We call ϕ an environment-context extractor. We define the optimal environment-context extractor ϕ^* the one that satisfies: $\exists \pi_{\phi^*} \in \Pi, \forall \rho \in \mathcal{T}, J_\rho(\pi_{\phi^*}) = \max_\pi J_\rho(\pi)$, where $\pi_\phi := \pi_\phi(a_t|\phi(z_t|\rho_t), s_t)$ is an adaptive policy and Π denotes the policy class. Since the dynamics can be changed, we use subscript ρ_t to denote the dynamics model at time-step t. We discuss the input of ϕ in the next section. Besides, we define the optimal adaptive policy $\pi^*_{\phi^*}$ the one that satisfies $\forall \rho \in \mathcal{T}, J_\rho(\pi^*_{\phi^*}) = \max_\pi J_\rho(\pi)$. With the optimal ϕ^* and $\pi^*_{\phi^*}$, given any ρ in $\mathcal{T}$, the adaptive policy can adapt to make the best decisions via the output of environment-context z. To achieve this, given a dynamics model set $\mathcal{T}$, we optimize ϕ and π_ϕ by the following objective function:

$$\phi^*, \pi^*_{\phi^*} = \arg\max_{\phi, \pi_\phi} \mathbb{E}_{\rho \sim \mathcal{T}} \left[J_\rho(\pi_\phi) \right]. \tag{1}$$

When deployed in the real-world ρ^r, OapRS infers the environment contexts by $\phi^*(\rho^r_t)$ and makes the best action by $\pi^*_{\phi^*}$. If all the variant of dynamics models in the real-world $\mathcal{T}_r$ fall into $\mathcal{T}$, we can deploy the policy robustly via the optimal ϕ^* and $\pi^*_{\phi^*}$.

To learn the robust ϕ^* and $\pi^*_{\phi^*}$ for real-world deployment, the crucial problem is to construct a set of dynamics $\{\rho\}$ to cover the real-world dynamics set $\mathcal{T}_r$. One ideal solution is to construct all possible dynamics model in $\mathcal{S} \times \mathcal{A} \times \mathcal{S}$ (or all possible context vectors in $\mathcal{Z}$ and the corresponding simulators when we have the knowledge of the environment context) and optimize ϕ and π via equation 1 (Tobin et al., 2017; Sadeghi & Levine, 2017; Tobin et al., 2018; James et al., 2019; Peng et al., 2018; Akkaya et al., 2019). However, in real-world applications like SRS, we have no exact knowledge to formulate customer behavior, and thus space $\mathcal{Z}$ is unknown. Besides, since the real-world fall in a subspace of the dynamics space, constructing all possible dynamics model directly is costly and inefficient for policy learning. We propose to regard model-learning algorithms G as an efficient generator to map dataset to a dynamics model where the latent environment-context is near the real-world: $G(\mathcal{D}) \to \rho$ (although does not match exactly). Then we construct a diverse dynamics set by augmenting on G and $\mathcal{D}$. In particular, for augmenting on $\mathcal{D}$, we divide the offline dataset by the domain knowledge (e.g., we can split the dataset by city, country, or time period in production recommendation systems); for augmenting on G, we can select several model-learning algorithms or different hyper-parameters for the same algorithm (Kurutach et al., 2018) to generate simulators.

We list the OapRS framework in Algorithm 1. The framework is robust to the distortion of simulators since our goal is to generate a dynamics model in which the environment contexts are near the

Algorithm 1 OapRS framework

Input: ϕ_φ as environment-context extractor, parameterized by φ; Adaptive policy network π_θ parameterized by θ; Offline expert data $\mathcal{D}$; Model learning algorithm G; Rollout horizon H;minibatch m for policy training
Process:

divide offline dataset into N partitions $\{\bar{\mathcal{D}}\}$ and generate $M \times N$ dynamics model $\{\rho\}$ by ensemble of M model learning technique G
for 1, 2, 3, ... **do**
  random select the dynamics model ρ^i in $\{\rho\}$ and sample s_1 from $\bar{\mathcal{D}}$ which is used to train ρ^i
  initialize buffer $\mathcal{D}_{rollout}$
  for t=1,2,...,H **do**
    sample z_t from $\phi(z_t|\rho_t^i)$ and then sample a_t from $\pi(a_t|s_t, z_t)$
    rollout one step $s_{t+1}, r_{t+1} \sim \rho_t^i(s_t, a_t)$ and then add $(s_{t+1}, r_{t+1}, s_t, a_t, z_t)$ to $\mathcal{D}_{rollout}$
    if $t \mod m == 0$ **then**
      Update ϕ and π with equation 1 by policy gradient (e.g., PPO) and then $\mathcal{D}_{rollout} \leftarrow \emptyset$
    end if
  end for
end for

distribution of the real-world instead of recovering the real-world dynamics exactly. The method is also robust to stochastic environments since it learns to adapt to all possible situations in the state out of the consistency region instead of doing penalty in the state with multiple situations. (as illustrated in Figure 1(b)). Additionally, we point out that the framework is orthogonal to other techniques since the reliable model-learning methods can reduce the requirement of dynamics augmentation to cover the real-world parameter space.

4.2 Optimization of Adaptive policy with environment-context extractor

In this section, we formulate the environment-context representation problem in SRS. We first define an environment-context dependent dynamics as follows: $\rho(s_{t+1}|s_t, a_t, z_t)$, where z is the environment-context vector. Before learning the representation z by $\phi(z|\rho)$, the question is: What is an suitable input to ϕ for representation learning.

In the SRS scenario, the recommendation policy interacts with customers in multiple domains. Each domain consists of numerous customers. Taking the ride-hailing platform as an example, the platform provides services in multiple cities (i.e., domains), and interacts with numerous drivers in each city (i.e., customers). To train a platform recommendation policy for customers, we regard each customer as an environment ρ. Different from traditional agent controlling, in SRS, customer's behavior is not only dependent on the character, but the domain he/she belongs to. For instance, passengers' demand will be very different with time and cities geographically. Drivers in different cities might have different engagement (i.e., online time) due to different demand and supply, which is independent of their personas. Drivers' behavior will also change when the domain he/she belongs to changes. Based on the analysis, we propose that the input of ϕ should include personas information besides domain information.

In the robotics domain, environment representation approaches, called system identification, have been proposed recently (Peng et al., 2018; Akkaya et al., 2019; Yu et al.). The policy incorporates an online system identification module $\phi(z_t|s_t, \tau_{0:t})$, which utilizes a history of past states and actions $\tau_{0:t} = [s_0, a_0, ..., s_{t-1}, a_{t-1}, s_t]$ to predict the parameters of the dynamics. Since ρ in SRS is also dependent on domain information, we follow the system identification technique and add the domain trajectory information $\mathcal{T}_{0:t} = [S_0, A_0, S_1, A_1, ..., S_t]$ to the input. That is: $z_t = \phi(s_t, a_{t-1}, S_t, A_{t-1}, z_{t-1})$, where $(S_t^d, A_{t-1}^d) := \{(s_t^{i,d}, a_{t-1}^{i,d})\}_{i=1}^N$, which includes N state-action pairs at each time-step t. We use superscript d to denote the domain type.

Since the number of customers N can be large and vary from timestep to timestep, it is impractical to feed (S_t^d, A_{t-1}^d) to the neural network directly. In this work, we propose State-Action Distributional variational AutoEncoder (SA-DAE) to solve this problem by inferring the latent embedding υ of X. In the rest of this article, we use $X_t^d := (S_t^d, A_{t-1}^d)$ to for brevity. We first design the data generative

process based on the encoded variable υ based on the two assumptions: First, we assume state-action pairs in X_t^d are i.i.d. sampled from a distribution $p_{\psi_t^d}(s,a)$, which is parameterized by ψ_t^d for each time-step t and domain d. Second, we also assume that the parameters ψ of the distribution are generated by a distribution $p_\theta(\psi|\upsilon)$, parameterized by θ. It involves a latent continuous random variable υ, which is generated from another prior distribution $p(\upsilon)$. Then the generation of X includes three steps: (1) sample υ from $p(\upsilon)$; (2) sample ψ from distribution $p_\theta(\psi|\upsilon)$; (3) sample $p_\psi(s,a)$ repeatedly to generate X.

Our target is to learn an embedding model $q_\kappa(\upsilon|X)$ parameterized by κ, aligned with the posterior approximation $p_\theta(\upsilon|X)$. Using Kullback-Leibler Divergence (KLD) as the measurement, the objective can be written as follows:

$$\min L_{\mathbf{dae}} = \min \mathbb{E}_{X\sim\mathcal{D}_X}\left[KLD\left(q_\kappa(\upsilon|X)||p_\theta(\upsilon|X)\right)\right], \tag{2}$$

where the dataset $\mathcal{D}_X := \{X_t^d : d \in \mathcal{G}, 0 < t \leq T\}$ includes state-action pairs in all time-steps $0 < t \leq T$ and domains $\mathcal{G}$, and the posterior $p_\theta(\upsilon|X)$ is the target distribution of $q_\kappa(\upsilon|X)$. Under the assumption of i.i.d. sampling on X, the probabilities of $q_\kappa(\upsilon|X)$ and $p_\theta(X|\upsilon)$ can be estimated via likelihood:

$$q_\kappa(\upsilon|X) = \prod_{i=1}^{N} q_\kappa\left(\upsilon|s^{(i)}, a^{(i)}\right) \tag{3}$$

$$p_\theta(X|\upsilon) = \prod_{i=1}^{N} p_\theta\left(s^{(i)}, a^{(i)}|\upsilon\right) = \prod_{i=1}^{N} p_\psi\left(s^{(i)}, a^{(i)}\right) p_\theta(\psi|\upsilon), \tag{4}$$

where ψ denotes the parameters of distribution p_ψ. We give our theorem on the tractable evidence lower bound (ELBO) in Theorem 1. We leave the proofs in the Appendix A.

Theorem 1 *The tractable ELBO of state-action distributional variational inference is:*

$$\mathbb{E}_{X\sim\mathcal{D}_X}\left[\mathbb{E}_{q_\kappa(\upsilon|X)}\left[\sum_{i=1}^{N}\log p_\theta\left(s^{(i)}|\upsilon\right) + \log p_\theta\left(a^{(i)}|\upsilon, s^{(i)}\right)\right] + KLD\left(q_\kappa(\upsilon|X)||p_\theta(\upsilon)\right)\right] \tag{5}$$

Theorem 1 give us a three-step pipeline to minimize the objective of equation 2: (1) sample a batch of $X = \{(s,a)\}$ from expert dataset $\mathcal{D}_X$; (2) infer latent code υ via the likelihood probability of equation 3; (3) compute the reconstructed log-probability of state-action pairs based on equation 4 and KL divergence between posterior and prior of υ, and then apply the gradient to κ and θ.

Finally, the function q_κ embed the distribution of customer trajectory $\mathcal{T}_{0:t}$ into the latent code trajectory $\upsilon_{0:t}$. After that, the extractor ϕ can infer environment-context both with υ and τ. Then the adaptive policy $\pi\left(a_t \mid s_t, z_t\right)$ samples an action based on z_t.

4.3 ROBUST OFFLINE POLICY AND MODEL LEARNING IN IMPLEMENTATION

The dynamics model and policy are high-dimensional and complex to learn. We introduce three important implementation techniques to handle these problems (more details can be found in the Appendix F): (1) Semi dynamics model learning: To reduce the model learning complexity, with domain expert knowledge, we learn the $\pi^h(\bar{s}|s,a)$ and use a hand-coded function $map(s'|\bar{s},s,a)$ to construct the left of the states, instead of learning to predict s' directly; (2) Confidence penalty: To reduce the cost of dynamics model construction, we send policy with a large negative reward when policy reach the unreal regions. The unreal region is judged by a expert rule. (3) Domain reward normalization: Reward normalization is important for model-free RL algorithms (Engstrom et al.). However, different simulators may have different reward scales. Instead of rescaling the reward with a uniform scale, we rescale the reward for each domain.

5 EXPERIMENTS

In this work, we focus on the three research questions: (1) In SRS scenarios, can the adaptive policy of OapRS make more robust decisions than other learn-to-adapt methods do? (2) By adapting to the learned representation of the dynamics, can OapRS handle the distortion of the constructed dynamics models? (3) Does non-steadiness and stochasticity in real-world applications actually affect the performance of offline learning? If so, does OapRS overcome this challenge? We conduct experiments in a synthetic environment and a real-world environment to answer these questions.

5.1 RESULTS IN SYNTHETIC ENVIRONMENT

To analyze the adaptability of OapRS and its robustness to distortion, we first conduct the experiments in a synthetic environment in which the environment parameters z are configurable. The environment is called the long-term customer satisfaction (LTS) problem, a sequential recommendation environment comes from Google RecSim (Ie et al., 2019). Instead of constructing dynamics set by learning with augmentation (line 1 in Algorithm 1), for analyzing the results reasonably, we construct the training dynamics set by selecting z directly, and control the difference of z between the training set and the target domain to design different tasks. In particular, we construct the target dynamics with z^{test} and select the training dynamics set by equidistant sampling parameters z from the space and removing those $||z - z^{test}|| < \alpha$. The details of environment and experiment setup of the following can be found in Appendix B.1.

We first test the adaptability of OapRS in SRS. The algorithms we compared are (1) DR-UNI: The domain randomization technique to learn a uniform policy ((Tobin et al., 2017)); (2) DR-OSI: An online system identification algorithm proposed by Peng et al. (2018); (3) DIRECT: Train in the dynamics model where z nearest to the target domain and deploy directly. (4) Upper Bound: A policy trained in the target domain directly. We regarded it as the upper bound performance. We construct three tasks: "LTS1", "LTS2" and "LTS3". The numbers after "LTS" denote the removing scale α. We report our results in Figure 2. First, the results of DIRECT show that the performance degradation is severe in the tasks. Without considering the difference between training and deploying, the policy generates unpredictable behaviors. Second, all algorithms which consider learning from multiple dynamic models can improve the robustness in unknown domains. However, the algorithms that adapt by the representation of environments (OapRS and DR-OSI) reach better performance since they try to find the optimal policy in the representation of the environment instead of maximizing the expected performance in the training set. In addition, OapRS reaches the near-optimal performance and does better than DR-OSI in difficult tasks (e.g., LTS3). The results demonstrate that without considering the domain information, the representation can not be extracted well. In more difficult tasks, the limitation of the representation ability restricts the performance of the adaptive policy. We show more results about the SA-DAE and the extractor in Appendix C.

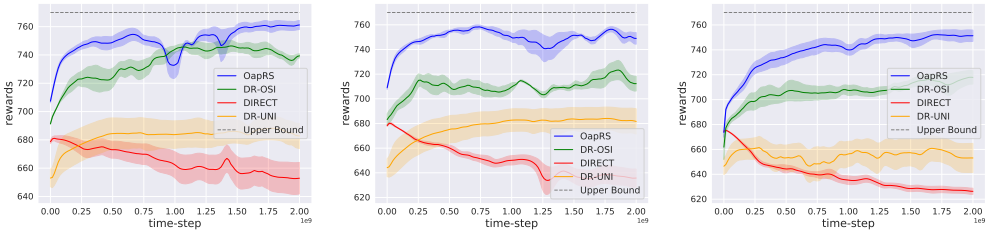

(a) LTS1 (b) LTS2 (c) LTS3

Figure 2: Illustration of the performance in synthetic environments. The solid curves are the mean reward and the shadow is the standard error of three seeds.

We then analyze the influence of dynamics distortion on OapRS. To mimic the process of offline model-based learning, we follow the previous experiment setting at "LTS3", but divide z into two part: z_e and z_d. In particular, z_e denotes the parameters that the behavior can be learned well by dynamics model, which are equidistant sampled as before. And z_d denotes the distortion parameters, which are the same in all dynamic models if distortion does not exist. We generate the distorted dynamics parameter $\hat{z_d}$ by $\hat{z_d} \sim z_d + U(-\beta, \beta)$ for training, where β can be regarded as the level of distortion. Figure 3 shows the performance of OapRS in this setting. We can see in Figure 3(a) that the deployment performance of OapRS with limited training set declines when the distortion level becomes larger, but the performance is still better than the compared methods. However, in Figure 3(b), we found that with enough sampled simulators, OapRS can overcome the distortion problem well. As a conclusion, in empirically, by augmenting enough diverse dynamics models, it is possible to overcome the distortion problem via OapRS.

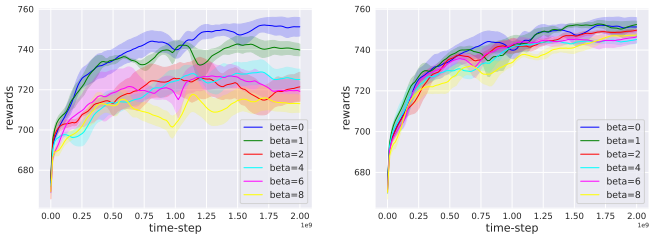

(a) limited simulators (b) unlimited simulators

Figure 3: Illustration of the performance in distored synthetic environments. The solid curves are the mean reward and the shadow is the standard error of three seeds. In limited setting, we sample β for each simulator and fix it. In unlimited setting, we sample β for each simulator and each episode.

5.2 Experiments in a Real-World Application

We finally test OapRS in the driver program recommendation (DPR) of a large-scale ride-hailing platform in the real world (the detail of task setting can be seen Appendix B.2). The offline data comes from a human policy. We construct the dynamics model set by DEMER (Shang et al., 2019) for its ability to learn hidden confounders. For dynamics model augmentation, we divide the dataset into 34 partitions by cities and time periods. For better comparison of algorithms and demonstrate the offline learning performance in stochastic environments, we first conduct a semi-online experiment: We leave one city in the dynamics set out for policy training, and test the policy performance in the unseen city. We select three different cities for these experiments. The algorithms we compare are: (1) MOPO: an offline model-based algorithm by consistency penalties. The dynamics models are also trained by DEMER (Yu et al., 2020); (2) BCQ: an offline model-free algorithm by constraining actions (Wang et al., 2020). Figure 4(a), Figure 4(b) and Figure 4(c) show the results. We finally deploy the policy trained by MOPO and OapRS to the real-world and test the performance for 7 days. The results is shown in Figure4(d). We deploy the policy from day 23 to day 29. Before deployment, drivers are recommended with the same human expert policy. We found that the performance improvement of the MOPO policy is 0.1%, which is similar to the expert policy, while the improvement of OapRS is 6.9%, which is significantly better than the expert. The details of the results can be seen in Table 3.

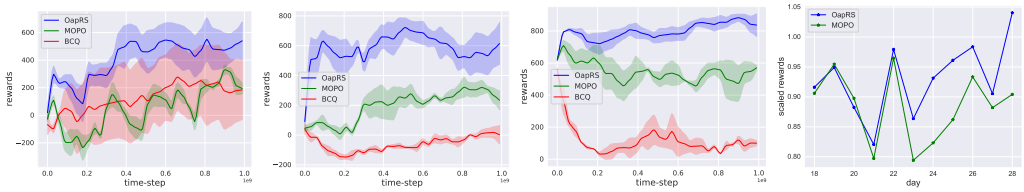

(a) City A (semi-online) (b) City B (semi-online) (c) City C (semi-online) (d) City A online

Figure 4: Illustration of the performance in semi-online and online tests. In the semi-online setting, the Y-axis is the averaged long-term reward among the users in the environments. In the online test, the Y-axis is the averaged daily reward. The rewards of online data are rescaled.

6 Discussion

In this paper, we propose a new paradigm of model-based learning to solve the offline RL in real-world applications. We focus on two realistic problems in real-world SRS applications: (1) real-world environments are non-stationary; (2) real-world environments are often with stochasticity. Instead of learning by penalty, constraint or randomization, OapRS solves the problem by learning to adapt to diverse simulators generated by the offline dataset. We formulate and analyze the environment-parameter representation learning problem in SRS and optimize the adaptive policy with the learned environment representation. The experiment results show the adaptability of OapRS, the performance decline of offline RL algorithms faced with the two realistic problems, and how OapRS work well in this situation. Although we focus on the real-world application of SRS, we consider that OapRS can be a general paradigm to solve the offline RL problem in other complex environments.

REFERENCES

Rishabh Agarwal, Dale Schuurmans, and Mohammad Norouzi. An optimistic perspective on offline reinforcement learning. *International Conference on Machine Learning*, 2020.

Ilge Akkaya, Marcin Andrychowicz, Maciek Chociej, Mateusz Litwin, Bob McGrew, Arthur Petron, Alex Paino, Matthias Plappert, Glenn Powell, Raphael Ribas, Jonas Schneider, Nikolas Tezak, Jerry Tworek, Peter Welinder, Lilian Weng, Qiming Yuan, Wojciech Zaremba, and Lei Zhang. Solving rubik's cube with a robot hand. *CoRR*, abs/1910.07113, 2019.

Greg Brockman, Vicki Cheung, Ludwig Pettersson, Jonas Schneider, John Schulman, Jie Tang, and Wojciech Zaremba. Openai gym. *CoRR*, abs/1606.01540, 2016.

Han Cai, Kan Ren, Weinan Zhang, Kleanthis Malialis, Jun Wang, Yong Yu, and Defeng Guo. Real-time bidding by reinforcement learning in display advertising. In *Proceedings of the 10th. ACM International Conference on Web Search and Data Mining*, Cambridge, United Kingdom, 2017.

Logan Engstrom, Andrew Ilyas, Shibani Santurkar, Dimitris Tsipras, Firdaus Janoos, Larry Rudolph, and Aleksander Madry. Implementation matters in deep RL: A case study on PPO and TRPO. In *Proceeding of 8th. International Conference on Learning Representations*, Addis, Ethiopia.

Gene H. Golub and Charles F. Van Loan. *Matrix Computations (3rd Ed.)*. Johns Hopkins University Press, USA, 1996. ISBN 0801854148.

Tuomas Haarnoja, Aurick Zhou, Pieter Abbeel, and Sergey Levine. Soft Actor-Critic: Off-policy maximum entropy deep reinforcement learning with a stochastic actor. In *Proceedings of the 35th. International Conference on Machine Learning*, pp. 1856–1865, Stockholmsmässan, Sweden, 2018.

Nicolas Heess, Gregory Wayne, David Silver, Timothy P. Lillicrap, Tom Erez, and Yuval Tassa. Learning continuous control policies by stochastic value gradients. In Corinna Cortes, Neil D. Lawrence, Daniel D. Lee, Masashi Sugiyama, and Roman Garnett (eds.), *Advances in Neural Information Processing Systems 28: Annual Conference on Neural Information Processing Systems 2015*, Montreal, Canada.

Sepp Hochreiter and Jürgen Schmidhuber. Long short-term memory. *Neural Computation*, 9(8): 1735–1780, 1997.

Eugene Ie, Chih-Wei Hsu, Martin Mladenov, Vihan Jain, Sanmit Narvekar, Jing Wang, Rui Wu, and Craig Boutilier. RecSim: A configurable simulation platform for recommender systems. *CoRR*, abs/1909.04847, 2019.

Stephen James, Paul Wohlhart, Mrinal Kalakrishnan, Dmitry Kalashnikov, Alex Irpan, Julian Ibarz, Sergey Levine, Raia Hadsell, and Konstantinos Bousmalis. Sim-to-Real via Sim-to-Sim: Data-efficient robotic grasping via randomized-to-canonical adaptation networks. In *2019 IEEE Conference on Computer Vision and Pattern Recognition*, pp. 12627–12637, Long Beach, CA, 2019.

Lukasz Kaiser, Mohammad Babaeizadeh, Piotr Milos, Blazej Osinski, Roy H. Campbell, Konrad Czechowski, Dumitru Erhan, Chelsea Finn, Piotr Kozakowski, Sergey Levine, Afroz Mohiuddin, Ryan Sepassi, George Tucker, and Henryk Michalewski. Model based reinforcement learning for Atari. In *Proceeeding of the 8th. International Conference on Learning Representations*, Addis Ababa, Ethiopia, 2020.

Rahul Kidambi, Aravind Rajeswaran, Praneeth Netrapalli, and Thorsten Joachims. MOReL : Model-based offline reinforcement learning. *CoRR*, abs/2005.05951, 2020.

David Krueger, Tegan Maharaj, Shane Legg, and Jan Leike. Misleading meta-objectives and hidden incentives for distributional shift. *Safe Machine Learning workshop at ICLR*, 2019.

Aviral Kumar, Justin Fu, Matthew Soh, George Tucker, and Sergey Levine. Stabilizing off-policy q-learning via bootstrapping error reduction. In Hanna M. Wallach, Hugo Larochelle, Alina Beygelzimer, Florence d'Alché-Buc, Emily B. Fox, and Roman Garnett (eds.), *Advances in Neural Information Processing Systems 32: Annual Conference on Neural Information Processing Systems 2019*, Vancouver, Canada, 2019.

Thanard Kurutach, Ignasi Clavera, Yan Duan, Aviv Tamar, and Pieter Abbeel. Model-ensemble trust-region policy optimization. In *Proceeding of 6th. International Conference on Learning Representations*, Vancouver, Canada, 2018.

Sascha Lange, Thomas Gabel, and Martin A. Riedmiller. Batch reinforcement learning. In Marco A. Wiering and Martijn van Otterlo (eds.), *Reinforcement Learning*, volume 12 of *Adaptation, Learning, and Optimization*, pp. 45–73. Springer, 2012.

Sergey Levine, Peter Pastor, Alex Krizhevsky, Julian Ibarz, and Deirdre Quillen. Learning hand-eye coordination for robotic grasping with deep learning and large-scale data collection. *The International Journal of Robotics Research*, 37(4-5):421–436, 2018.

Sergey Levine, Aviral Kumar, George Tucker, and Justin Fu. Offline reinforcement learning: Tutorial, review, and perspectives on open problems. *CoRR*, abs/2005.01643, 2020.

Yao Liu, Adith Swaminathan, Alekh Agarwal, and Emma Brunskill. Off-policy policy gradient with state distribution correction. *CoRR*, abs/1904.08473, 2019.

Yuping Luo, Huazhe Xu, Yuanzhi Li, Yuandong Tian, Trevor Darrell, and Tengyu Ma. Algorithmic framework for model-based deep reinforcement learning with theoretical guarantees. In *Proceeding of 7th. International Conference on Learning Representations, ICLR 2019, New Orleans, LA, USA, May 6-9, 2019*, New Orleans, LA, 2019.

Anusha Nagabandi, Ignasi Clavera, Simin Liu, Ronald S. Fearing, Pieter Abbeel, Sergey Levine, and Chelsea Finn. Learning to adapt in dynamic, real-world environments through meta-reinforcement learning. In *Proceeding of 7th. International Conference on Learning Representations*, New Orleans, LA.

Xue Bin Peng, Marcin Andrychowicz, Wojciech Zaremba, and Pieter Abbeel. Sim-to-Real transfer of robotic control with dynamics randomization. In *Proceedings of the 35th. IEEE International Conference on Robotics and Automation*, pp. 1–8, Brisbane, Australia, 2018.

Kate Rakelly, Aurick Zhou, Chelsea Finn, Sergey Levine, and Deirdre Quillen. Efficient off-policy meta-reinforcement learning via probabilistic context variables. In *Proceedings of the 36th. International Conference on Machine Learning*, pp. 5331–5340, Long Beach, CA, 2019.

Murray Rosenblatt. Remarks on some nonparametric estimates of a density function. *Annals of Mathematical Statistics*, 27(3):832–837, 09 1956.

Fereshteh Sadeghi and Sergey Levine. CAD2RL: Real single-image flight without a single real image. In *Proceedings of the 13rd. Robotics: Science and Systems, Massachusetts Institute of Technology*, Cambridge, MA, 2017.

Fereshteh Sadeghi, Alexander Toshev, Eric Jang, and Sergey Levine. Sim2Real viewpoint invariant visual servoing by recurrent control. In *2018 IEEE Conference on Computer Vision and Pattern Recognition*, Salt Lake City, UT.

John Schulman, Sergey Levine, Pieter Abbeel, Michael I. Jordan, and Philipp Moritz. Trust region policy optimization. In *Proceedings of the 32nd. International Conference on Machine Learning*, pp. 1889–1897, Lille, France, 2015.

John Schulman, Filip Wolski, Prafulla Dhariwal, Alec Radford, and Oleg Klimov. Proximal policy optimization algorithms. *CoRR*, abs/1707.06347, 2017.

Wenjie Shang, Yang Yu, Qingyang Li, Zhiwei Qin, Yiping Meng, and Jieping Ye. Environment reconstruction with hidden confounders for reinforcement learning based recommendation. In *Proceedings of the 25th. ACM SIGKDD International Conference on Knowledge Discovery & Data Mining*, pp. 566–576, Anchorage, AK, 2019.

Noah Y. Siegel, Jost Tobias Springenberg, Felix Berkenkamp, Abbas Abdolmaleki, Michael Neunert, Thomas Lampe, Roland Hafner, Nicolas Heess, and Martin A. Riedmiller. Keep doing what worked: Behavior modelling priors for offline reinforcement learning. In *Proceeding of the 8th. International Conference on Learning Representations*, Addis Ababa, Ethiopia.

Alexander L. Strehl, Lihong Li, Eric Wiewiora, John Langford, and Michael L. Littman. PAC model-free reinforcement learning. In *Machine Learning, Proceedings of the 23rd. International Conference*, pp. 881–888, Pennsylvania, PA, 2006.

Richard S. Sutton and Andrew G. Barto. *Reinforcement Learning: An Introduction*. MIT Press, 2018.

Josh Tobin, Rachel Fong, Alex Ray, Jonas Schneider, Wojciech Zaremba, and Pieter Abbeel. Domain randomization for transferring deep neural networks from simulation to the real world. In *Proceedings of the 29th. IEEE/RSJ International Conference on Intelligent Robots and Systems*, pp. 23–30, Vancouver, Canada, 2017.

Josh Tobin, Lukas Biewald, Rocky Duan, Marcin Andrychowicz, Ankur Handa, Vikash Kumar, Bob McGrew, Alex Ray, Jonas Schneider, Peter Welinder, Wojciech Zaremba, and Pieter Abbeel. Domain randomization and generative models for robotic grasping. In *2018 IEEE/RSJ International Conference on Intelligent Robots and Systems*, pp. 3482–3489, Madrid, Spain, 2018.

Emanuel Todorov, Tom Erez, and Yuval Tassa. MuJoCo: A physics engine for model-based control. In *Proceedings of the 24th. IEEE/RSJ International Conference on Intelligent Robots and Systems*, pp. 5026–5033, Vilamoura, Portugal, 2012.

Ulrich Viereck, Andreas ten Pas, Kate Saenko, and Robert Platt Jr. Learning a visuomotor controller for real world robotic grasping using simulated depth images. In *Proceedings of the 1st. Annual Conference on Robot Learning*, pp. 291–300, Mountain View, CA, 2017.

Chengwei Wang, Tengfei Zhou, Chen Chen, Tianlei Hu, and Gang Chen. Off-policy recommendation system without exploration. In Hady W. Lauw, Raymond Chi-Wing Wong, Alexandros Ntoulas, Ee-Peng Lim, See-Kiong Ng, and Sinno Jialin Pan (eds.), *Advances in Knowledge Discovery and Data Mining - 24th Pacific-Asia Conference*, Singapore, 2020.

Tingwu Wang, Xuchan Bao, Ignasi Clavera, Jerrick Hoang, Yeming Wen, Eric Langlois, Shunshi Zhang, Guodong Zhang, Pieter Abbeel, and Jimmy Ba. Benchmarking model-based reinforcement learning. *CoRR*, abs/1907.02057, 2019.

Xiting Wang, Yiru Chen, Jie Yang, Le Wu, Zhengtao Wu, and Xing Xie. A reinforcement learning framework for explainable recommendation. In *2018 IEEE International Conference on Data Mining*, pp. 587–596. IEEE, 2018.

Svante Wold, Kim Esbensen, and Paul Geladi. Principal component analysis. *Chemometrics and intelligent laboratory systems*, 2(1-3):37–52, 1987.

Yifan Wu, George Tucker, and Ofir Nachum. Behavior regularized offline reinforcement learning. *CoRR*, abs/1911.11361, 2019.

Tianhe Yu, Garrett Thomas, Lantao Yu, Stefano Ermon, James Zou, Sergey Levine, Chelsea Finn, and Tengyu Ma. MOPO: model-based offline policy optimization. *CoRR*, abs/2005.13239, 2020.

Wenhao Yu, Jie Tan, C. Karen Liu, and Greg Turk. Preparing for the unknown: Learning a universal policy with online system identification. In Nancy M. Amato, Siddhartha S. Srinivasa, Nora Ayanian, and Scott Kuindersma (eds.), *Robotics: Science and Systems XIII, Massachusetts Institute of Technology, , July 12-16, 2017*, Cambridge, MA.

Fangyi Zhang, Jürgen Leitner, Michael Milford, Ben Upcroft, and Peter I. Corke. Towards vision-based deep reinforcement learning for robotic motion control. *CoRR*, abs/1511.03791, 2015.

Xiangyu Zhao, Liang Zhang, Zhuoye Ding, Long Xia, Jiliang Tang, and Dawei Yin. Recommendations with negative feedback via pairwise deep reinforcement learning. In *Proceedings of the 24th. ACM SIGKDD International Conference on Knowledge Discovery & Data Mining*, London, UK.

Xiangyu Zhao, Changsheng Gu, Haoshenglun Zhang, Xiaobing Liu, Xiwang Yang, and Jiliang Tang. Deep reinforcement learning for online advertising in recommender systems. *CoRR*, abs/1909.03602, 2019. URL `http://arxiv.org/abs/1909.03602`.

Yuke Zhu, Ziyu Wang, Josh Merel, Andrei A. Rusu, Tom Erez, Serkan Cabi, Saran Tunyasuvunakool, János Kramár, Raia Hadsell, Nando de Freitas, and Nicolas Heess. Reinforcement and imitation learning for diverse visuomotor skills. In *Robotics: Science and Systems XIV*, Pittsburgh, PA, 2018.

A PROOF OF SA-DAE

We design the data generative process based on the encoded variable υ with two assumptions: First, we assume that state-action pairs in X are i.i.d. sampled from a distribution $p_\psi(s, a)$, which is parameterized by ψ. Second, we also assume that the distribution parameters ψ are generated by a distribution $p_\theta(\psi|\upsilon)$, parameterized by θ. It involves a latent continuous random variable υ, which is generated from another prior distribution $p(\upsilon)$. Then, the generation of X includes three steps: 1) sample υ from $p(\upsilon)$; 2) sample ψ from distribution $p_\theta(\psi|\upsilon)$; 3) sample $p_\psi(s, a)$ repeatedly to generate X. A comparison with VAE on directed graphical model is shown in Figure 5.

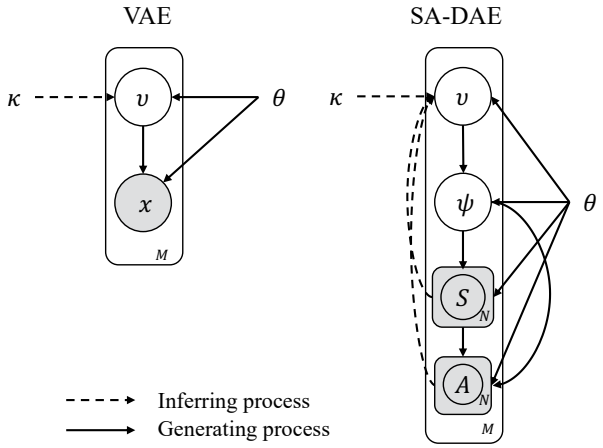

Figure 5: Comparison of SA-DAE and vanilla VAE through the directed graphical model. The circles denote the variable nodes. The rounded rectangle denotes the dataset nodes, in which the notation in the corner denotes the number of datasets. θ denotes the approximation parameters of the generative model, and κ denotes the parameters of the variational approximation model.

Our target is to learn an embedding model $q_\kappa(\upsilon|X)$ parameterized by κ, which aligned with the posterior $p_\theta(\upsilon|X)$. Using KL divergence (KLD) as the measure of distribution, the objective function can be written as follows:

$$\min L_{\mathbf{sad}} = \min \mathbb{E}_{X\sim\mathcal{D}_X}\left[KLD\left(q_\kappa(\upsilon|X)||p_\theta(\upsilon|X)\right)\right]. \tag{6}$$

where the dataset $\mathcal{D}_X := \{X_t^d : d \in \mathcal{G}, 0 < t \leq T\}$ includes state-action pairs in all time-steps $0 < t \leq T$ and domains $\mathcal{G}$, and the posterior $p_\theta(\upsilon|X)$ is the target distribution of $q_\kappa(\upsilon|X)$. We provide the evidence lower bound (ELBO) of Equation equation 6 in Lemma 1.

Lemma 1 *The ELBO of state-action distributional variational inference is:*

$$ELBO = \mathbb{E}_{X\sim\mathcal{D}_X}\left[\mathbb{E}_{q_\kappa(\upsilon|X)}\left[\log p_\theta(X|\upsilon)\right] - KLD\left(q_\kappa(\upsilon|X)||p_\theta(\upsilon)\right)\right]$$

Proof A.1

$$\begin{aligned}
& KLD(q_\kappa(\upsilon|X)||p_\theta(\upsilon|X)) && (7)\\
=&\mathbb{E}_{q_\kappa(\upsilon|X)}\left[\log\frac{q_\kappa(\upsilon|X)}{p_\theta(\upsilon|X)}\right]\\
=&\mathbb{E}_{q_\kappa(\upsilon|X)}\left[\log q_\kappa(\upsilon|X) - \log p_\theta(\upsilon, X) + \log p_\theta(X)\right]\\
=& -L(\theta, \kappa; X) + \log p_\theta(X), && (8)
\end{aligned}$$

Since $\log p_\theta(X)$ *is independent of* $q_\kappa(\upsilon|X)$*, minimizing Equation equation 7 is equivalent to maximize* $L(\theta, \kappa; X)$ *in Equation equation 8.*

Based on Bayes's theorem, we have:

$$\begin{aligned}L(\theta,\kappa;X)=&\mathbb{E}_{q_\kappa(\upsilon|X)}\left[-\log q_\kappa(\upsilon|X)+\log p_\theta(\upsilon,X)\right]\\=&\mathbb{E}_{q_\kappa(\upsilon|X)}\left[-\log q_\kappa(\upsilon|X)+\log\left(p_\theta(X|\upsilon)p_\theta(\upsilon)\right)\right]\\=&\mathbb{E}_{q_\kappa(\upsilon|X)}\left[\log\frac{p_\theta(\upsilon)}{q_\kappa(\upsilon|X)}+\log p_\theta(X|\upsilon)\right]\\=&\mathbb{E}_{q_\kappa(\upsilon|X)}\left[\log p_\theta(X|\upsilon)\right]-KLD\left(q_\kappa(\upsilon|X)||p_\theta(\upsilon)\right),\end{aligned}$$

Under the assumption that X is i.i.d. sampled from $\mathcal{D}_X$, we obtain the evidence lower bound (ELBO) objective:

$$\max\mathbb{E}_{X\sim\mathcal{D}_X}\left[\mathbb{E}_{q_\kappa(\upsilon|X)}\left[\log p_\theta(X|\upsilon)\right]-KLD\left(q_\kappa(\upsilon|X)||p(\upsilon)\right)\right].$$

Theorem 2 *The tractable ELBO of state-action distributional variational inference is:*

$$\mathbb{E}_{X\sim\mathcal{D}_X}\left[\mathbb{E}_{q_\kappa(\upsilon|X)}\left[\sum_{i=1}^{N}\log p_\theta\left(s^{(i)}|\upsilon\right)+\log p_\theta\left(a^{(i)}|\upsilon,s^{(i)}\right)\right]+KLD\left(q_\kappa(\upsilon|X)||p(\upsilon)\right)\right]\quad(9)$$

Proof A.2 *Under the assumption of i.i.d. sampling on X, the probability of $q_\kappa(\upsilon|X)$ and $p_\theta(X|\upsilon)$ can be estimated via likelihood:*

$$q_\kappa(\upsilon|X)=\prod_{i=1}^{N}q_\kappa\left(\upsilon|s^{(i)},a^{(i)}\right)\quad(10)$$

$$p_\theta(X|\upsilon)=\prod_{i=1}^{N}p_\theta\left(s^{(i)},a^{(i)}|\upsilon\right)=\prod_{i=1}^{N}p_\psi\left(s^{(i)},a^{(i)}\right)p_\theta(\psi|\upsilon),\quad(11)$$

where ψ denotes the parameters of distribution p_ψ.

In the reinforcement learning scenario, the action is sampled conditionally on the state, thus the posterior p_θ can be separated by:

$$\begin{aligned}&p_\theta\left(s^{(i)},a^{(i)}|\upsilon\right)\\=&p_\theta\left(a^{(i)}|\upsilon,s^{(i)}\right)p_\theta\left(s^{(i)}|\upsilon\right)\\=&p_{\psi_a}\left(a^{(i)}\right)p_\theta\left(\psi_a|\upsilon,s^{(i)}\right)p_{\psi_s}\left(s^{(i)}\right)p_\theta\left(\psi_s|\upsilon\right),\end{aligned}\quad(12)$$

where ψ_s and ψ_a denote the decoded parameters of the distribution. Then the trac ELBO objective can be written as:

$$\begin{aligned}&\mathbb{E}_{X\sim\mathcal{D}_X}\left[\mathbb{E}_{q_\kappa(\upsilon|X)}\left[\log p_\theta(X|\upsilon)\right]-KLD\left(q_\kappa(\upsilon|X)||p(\upsilon)\right)\right]\\=&\mathbb{E}_{X\sim\mathcal{D}_X}\left[\mathbb{E}_{q_\kappa(\upsilon|X)}\left[\sum_{i}^{N}\log p_\theta\left(x^{(i)}|\upsilon\right)\right]-KLD\left(q_\kappa(\upsilon|X)||p(\upsilon)\right)\right]\\=&\mathbb{E}_{X\sim\mathcal{D}_X}\left[\mathbb{E}_{q_\kappa(\upsilon|X)}\left[\sum_{i=1}^{N}\log p_\theta\left(s^{(i)}|\upsilon\right)+\log p_\theta\left(a^{(i)}|\upsilon,s^{(i)}\right)\right]+KLD\left(q_\kappa(\upsilon|X)||p(\upsilon)\right)\right].\end{aligned}$$

Since $q_\kappa\left(\upsilon|s^{(i)},a^{(i)}\right)$ can be modeled with Gaussian distribution, the results are also a Gaussian distribution Rakelly et al. (2019). Besides, $p_\theta\left(a^{(i)}|\upsilon,s^{(i)}\right)=p_{\psi_a}\left(a^{(i)}\right)p_\theta\left(\psi_a|\upsilon,s^{(i)}\right)$ and $p_\theta\left(s^{(i)}|\upsilon\right)=p_{\psi_s}\left(s^{(i)}\right)p_\theta\left(\psi_s|\upsilon\right)$, where ψ_s and ψ_a denote the decoded parameters of the distribution. Thus, for any differentiable p_{ψ_s} and p_{ψ_a}, the ELBO objective is tractable.

In summary, SA-DAE has a three-step pipeline to minimize the objective of Equation equation 9:

1. Sample a batch of X from the dataset $\mathcal{D}_X$;
2. Infer latent code υ via the likelihood probability based on Equation equation 10;
3. Compute the reconstructed log-probability of state-action pair based on Equation equation 12 and Equation equation 11, and compute the KL divergence between posterior and prior of υ, then apply the gradient with respect to κ and θ.

B EXPERIMENTAL SETTINGS

B.1 MULTIPLE-DOMAIN MULTIPLE-CUSTOMER LONG-TERM SATISFACTION PROBLEM (LTS)

Long-term satisfaction (Choc/Kale) problem comes from a synthetic environment in the Google RecSim framework Ie et al. (2019). In this environment, the recommendation system sends items of content to customers, and the goal is to maximize customers' engagement in multiple timesteps. The items of content are characterized by the score of clickbaitiness. The engagement of customers is determined by the clickbaitiness score of content and the long-term satisfaction score. The higher clickbaitiness score leads to a larger engagement directly but leads to a decrease in the long-term satisfaction while the lower clickbaitiness score increases satisfaction but leads to a smaller engagement directly. Moreover, the long-term satisfaction is a coefficient to rescale the engagement of the given item of content. In particular, the value of engagement for customer i at timestep t is sampled from a Gaussian distribution $\mathcal{N}\left(\mu_t^i, {\sigma_t^i}^2\right)$, which is parameterized by

$$\begin{aligned}\mu_t^i &:= \left(a_t^i \mu_c^i + \left(1 - a_t^i\right) \mu_k^i\right) SAT_t^i \\ \sigma_t^i &:= \left(a_t^i \sigma_c^i + \left(1 - a_t^i\right) \sigma_k^i\right),\end{aligned}$$

where i denotes the index of customer, a_t^i denotes the clickbaitiness score of the given item. μ_c^i, μ_k^i, σ_c^i and σ_k^i are hidden states of the customer i. SAT_t^i denotes the long-term satisfaction score, which is updated by a_t:

$$\begin{aligned}SAT_t^i &:= sigmoid\left(h_s^i \times NPE_t^i\right) \\ NPE_t^i &:= \gamma^i NPE_{t-1}^i - 2\left(a_t^i - 0.5\right),\end{aligned}$$

where NPE_t^i denotes the net positive exposure score of the customer i, γ^i denotes the memory discount of NPE_t^i, and h_s^i denotes the sensitivity ratio of NPE to satisfaction. γ^i and h_s^i are also hidden states in this environment.

For the LTS environment, the hidden states μ_c^i, μ_k^i, σ_c^i, σ_k^i, h_s^i and γ^i define customer behaviors. To construct the problem as the multiple-domain multiple-customer environment, we use μ_c^i to represent the parameter of group information z_d, which are the same among customers in the same simulator, and the rest of the hidden states are randomly sampled for each customer, to represent the parameter of z.

In our scenario, group-behavior parameters can only be identified through multiple customers' trajectories via an unkown projection function f, i.e., $z_d^t = f(\mathcal{T}_{0:t})$, where $\mathcal{T}_{0:t} = [S_0, A_0, ...S_{t-1}, A_{t-1}, S_t]$, and S and A denote the state and action sets of all customers in the same domain. To model this scenario in the synthetic environment, we need to design extra observations for each customer to infer z_d^t. We consider the simplest case: z_d is time-invariant and can be identified by S_t at any timestep t. In implementation, each customer has an extra fixed observation sampled from Gaussian distribution $o^i \sim \mathcal{N}(\mu_c, \omega_c)$. Then z_d is identifiable through multiple customers' observation, since $z_d = \mathrm{E}_i\left[o^i\right]$.

We construct the simulator in which $\mu_c = 14$ as the test simulator and select the training simulators by equidistant sampling parameters μ_c from environment-context space and removing those near the testing simulator. The observation of customers is sampled at $\omega_c = 4$. Then we construct three tasks with different transfer difficulties via controlling the removed range of parameters from training sets $\{\rho_{train}\}$:

- LTS1: $\{\rho_{train}\} = \{\rho_{\mu_c} : |\mu_c - 14| \geq 2 \wedge 6 \leq \mu_c < 22, \mu_c \in \mathbb{N}\}$
- LTS2: $\{\rho_{train}\} = \{\rho_{\mu_c} : |\mu_c - 14| \geq 3 \wedge 6 \leq \mu_c < 22, \mu_c \in \mathbb{N}\}$
- LTS3: $\{\rho_{train}\} = \{\rho_{\mu_c} : |\mu_c - 14| \geq 4 \wedge 6 \leq \mu_c < 22, \mu_c \in \mathbb{N}\}$

The environment-context space is set to $\mu_c \in [6, 22)$, taking 14 as the middle point, and we take the number of 2, 3 and 4 as the removed range for LTS1, LTS2 and LTS3, respectively.

In distortion test, we follow the setting of LTS3 and select μ_k as the distored parameter. In particular, for all simulators, $\mu_k^i \sim 4 + U(-\beta, \beta)$. Without considering distortion, μ_k^i is set to 4 for all customers in the simulators.

B.2 DRIVER PROGRAM SEQUENTIAL RECOMMENDATION PROBLEM

To demonstrate the effectiveness of the proposed method, we deploy OapRS in a real-world recommendation application, for a large-scale ride-hailing platform. The goal of the platform is to balance the demand from passengers and the supply of drivers, i.e., helping drivers finish more orders, and satisfying the more trip demand from passengers. The driver program recommendation (DPR) is one of the typical recommendation scenarios in the platform. In this scenario, to satisfy more demand from passengers, we would like to maximize the engagement of drivers via recommending reasonable items from the program. The engagement is characterized by the number of orders completed by each driver. The programs contain tasks for the driver to accomplish. If the driver completes the recommendation program, his/her engagement will increase. However, the difficulty of the task has influences on the completion rate since drivers respond differently to tasks, which also affects the effectiveness of recommendations. The responses are also changing for a driver over time. For example, the base number of demand is not in the same order of magnitude among the different cities, since the total passenger volumes vary. Hence, the drivers who have similar personas may behave differently in different cities, leading to diverse recommended programs.

The driver program recommendation can be modeled as an MDP. For simplification, we assume the influence among drivers can be ignored. It is reasonable since drivers almost have no ideas about other drivers' tasks. In the DPR environment, we regard each day as a timestep. At timestep t, the recommendation system policy π sends a program $a_t^i = \pi(s_t^i)$ to driver i based on the observed feature s_t^i. a_t^i denotes the program features to characterize the action. The reward r_t^i is the number of finished orders in the day. Our goal is to maximize the expectation of long-term engagement of drivers in different cities.

We divide real-world data into seventeen cities with two different periods for simulator learning. The Simulator is learned by technique Shang et al. (2019). Then the environment context is implied in the learned simulator models. In the semi-online test, we evaluate the policy performance with reality-gap via running the policy in the unseen city. The experiments allow testing the algorithms on the reality-gap through city and time period transfer, which is essentially environment context change.

C EXPERIMENTAL DETAILS IN LONG-TERM SATISFACTION PROBLEM

We first train a policy given oracle environment context in the synthetic simulators, to test the effect of the environment contexts. Figure 6 shows the action distribution of optimal policies in different contexts of μ_c. It can be seen that the larger μ_c leads to a larger percentage of the higher clickbaitiness-score item selected. Thus, a transferable policy should be aware of the differences of μ_c and adapt its decisions for better performance.

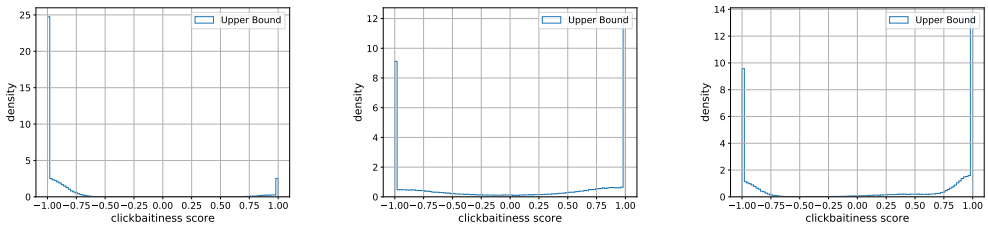

(a) $\mu_c = 6$ (b) $\mu_c = 14$ (c) $\mu_c = 21$

Figure 6: Illustration of generative action distribution for optimal policies in LTS3. The score is rescaled into $(-1, 1)$ from $(0, 30)$. We sample 750 trajectories of different customers and draw the histogram of these sampled actions.

In the LTS environment, z_d is only related to group state information S. Thus we train SA-DAE to reconstruct the state distribution instead of the state-action distribution. We draw 1000 customers for each simulator to the constructed state dataset $\mathcal{D}_X$. $q_\kappa\left(v|s^{(i)}\right)$ is a neural network which outputs the

Gaussian distribution parameters of υ. The dimension of vector υ is 5 in this environment. We also model $p_\theta(\psi_s|\upsilon)$ with a neural network, which outputs the parameters of Gaussian distributions. The prior of υ is set to standard normal distribution, i.e., $p(\upsilon) = \mathcal{N}(0, 1)$.

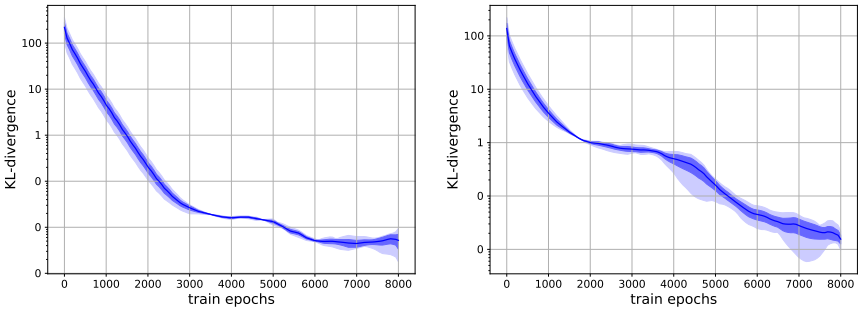

(a) KLD in training set (b) KLD in testing set

Figure 7: Illustration of KL divergence of the training set and testing set in LTS3. The solid curves are the mean reward of three seeds. The dark shadow is the standard error, and the light one is the min-max range of three seeds.

We use KLD to measure the performance of reconstruction. Since $p_\theta(\psi_s|\upsilon)$ also outputs the parameters of Gaussian distribution, we compute the KLD directly via the analytic expression of Gaussian distribution between $p_\theta(s|\upsilon)$ and $\mathcal{N}(\mu_c, \omega_c)$. We test the KLD every 100 epochs. Figure 7 shows that the KLD in the testing set finally converges to the range of 0.01 to 0.02. Figure 8 shows the reconstruction distribution is also correlated.

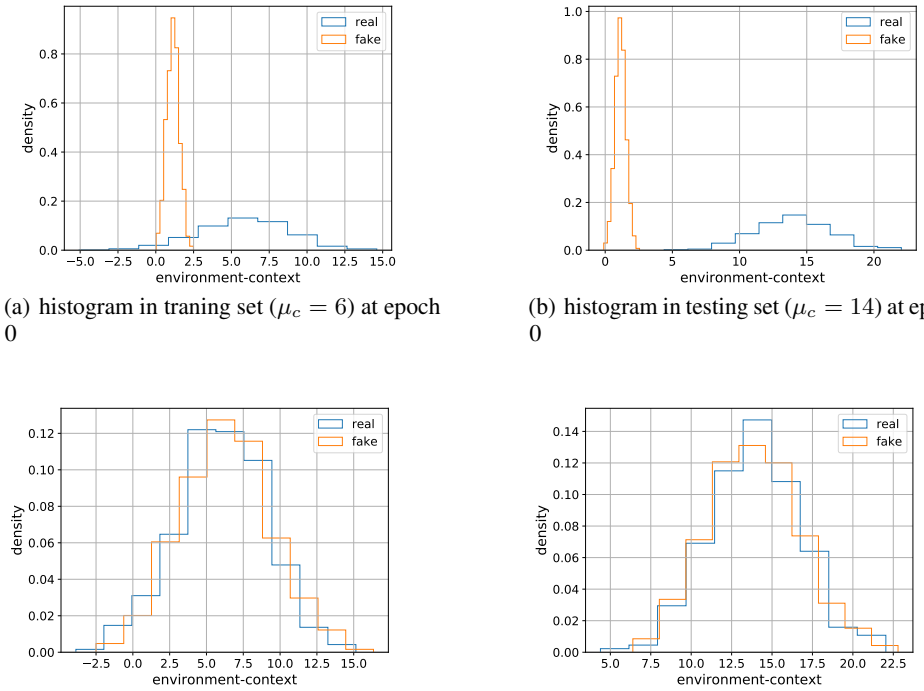

(a) histogram in traning set ($\mu_c = 6$) at epoch 0

(b) histogram in testing set ($\mu_c = 14$) at epoch 0

(c) histogram in traning set ($\mu_c = 6$) at epoch 8000

(d) histogram in testing set ($\mu_c = 14$) at epoch 8000

Figure 8: Illustration of the histogram about customer feature of o^i in reconstructed and real data in the task of LTS3.

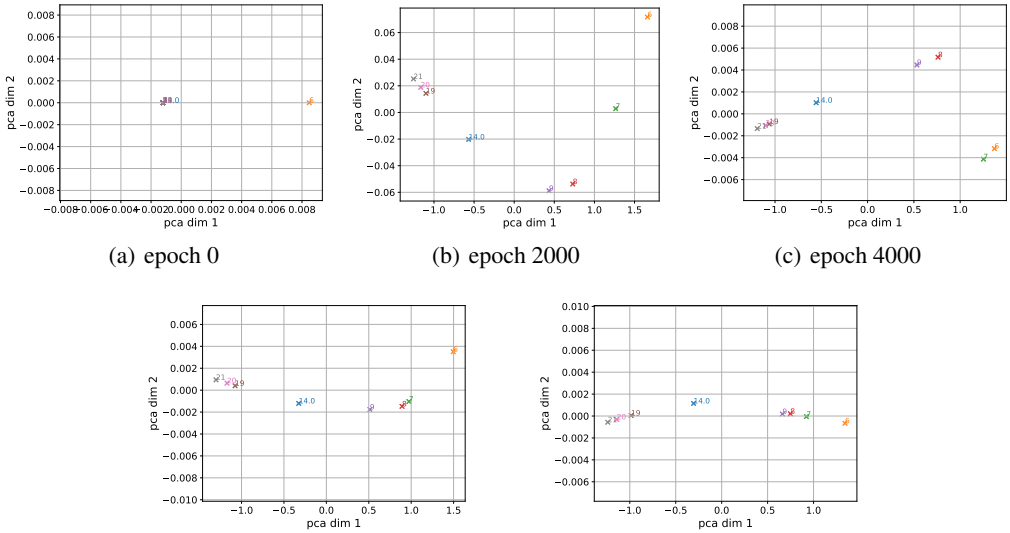

(a) epoch 0 (b) epoch 2000 (c) epoch 4000

(d) epoch 6000 (e) epoch 8000

Figure 9: Illustration of the visualization on υ. The X-axis denotes the first principal component, and the Y-axis denotes the second one. Each cross point denotes the projection of the latent code for the state distribution. The numbers with the same color to the point denote the ground-truth of μ_c. Although $q_\kappa(\upsilon|X)$ is a Gaussian distribution, we only draw the mean of the distribution for legibility.

To evaluate the embedding performance of SA-DAE, we project υ into two-dimensional vectors via principal component analysis (PCA) Wold et al. (1987). We show the result of PCA in Figure 9. It can be seen that, after 6000 epochs, the latent code can be represented by the first principal component. And the value of μ_c linearly depends on the first principal component.

We finally test the robustness of environment-parameter extractor to the noise scale ω_c. The result can be seen in Figure 10. The results show that the environment-parameter extractor can also work well in large noise ω_c situations.

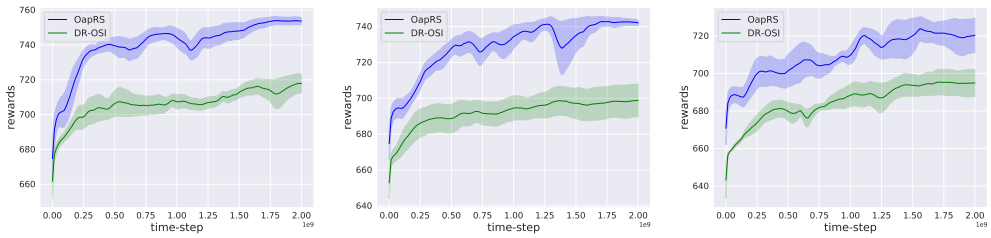

(a) $\omega_c = 4$ (b) $\omega_c = 10$ (c) $\omega_c = 14$

Figure 10: Illustration of the performance in synthetic environments in different ω_c. The solid curves are the mean reward and the shadow is the standard error of three seeds.

D PPO IMPLEMENTATION OF OAPRS

We use PPO Schulman et al. (2017) as an example and any policy-based methods (i.e., TRPO Schulman et al. (2015), SAC Haarnoja et al. (2018)) can also be plugged into the policy learning part. The pseudocode of OapRS is summarized in Algorithm 2.

Algorithm 2 OapRS implemented with PPO

Input:
Offline expert data $\mathcal{D}$;
LSTM network ϕ_φ as environment-context extractor, parameterized by φ
Adaptive policy network π_θ and value function network V_θ, parameterized by θ
Model learning algorithm G; Rollout horizon H;minibatch m for policy training
Training epochs M
Process:

Divide the offline dataset into N partitions $\{\bar{\mathcal{D}}\}$ and generate $M \times N$ dynamics model $\{\rho\}$ by ensemble of M model learning technique DEMER (Shang et al., 2019) G.
Pretrain the state-action distributional embedding model $q_\kappa(\upsilon|X)$ on $\{\bar{\mathcal{D}}\}$.
for 1, 2, 3, ... **do**
    random select the dynamics model ρ^i in $\{\rho\}$ and sample s_1 from $\bar{\mathcal{D}}$ which is used to train ρ^i
    initialize buffer $\mathcal{D}_{rollout}$
    for t=1,2,...,H **do**
        sample z_t from $\phi(z_t|\rho_t^i)$ and then sample a_t from $\pi(a_t|s_t, z_t)$
        rollout one step $s_{t+1}, r_{t+1} \sim \rho_t^i(s_t, a_t)$ and then add $(s_{t+1}, r_{t+1}, s_t, a_t, z_t)$ to $\mathcal{D}_{rollout}$
        if $t \mod m == 0$ **then**
            Compute the long-term reward estimates, $\hat{R}_t^{\pi_{\theta_m}}$, for each time-step t.
            Compute the advantage estimate, $\hat{A}_t^{\pi_{\theta_m}}$ based on the value function $V_\theta(s, z)$, where z is the output of extractor ϕ_φ.
            Compute the gradient ∇_θ and ∇_φ of the PPO objective :

$$\arg\max_{\theta,\varphi} \frac{1}{|\mathcal{D}_m|T} \sum_{\mathcal{T}\in\mathcal{D}_m} \sum_{t=0}^{T} q_\kappa(\upsilon_t|X_t) \sum_{s_t,a_{t-1},a_t,z_t\in\mathcal{T}} L_{PPO}(\theta, \varphi, \upsilon_t, s_t, a_t, a_{t-1}, z_t).$$

            Apply ∇_θ and ∇_φ.
            Update value function by one-step gradient of the regression loss:

$$\arg\min_{\theta} \frac{1}{|\mathcal{D}_m|T} \sum_{\mathcal{T}\in\mathcal{D}_m} \sum_{t=0}^{T} q_\kappa(\upsilon_t|X_t) \sum_{s_t,a_{t-1}\in\mathcal{T}} \left(V_\theta(s_t, z_t')\phi_\varphi(z_t'|z_{t-1}', s_t, a_{t-1}, \upsilon_t) - \hat{R}_t^{\pi_{\theta_m}}\right)^2$$

            Update the state-action distributional embedding model $q_\kappa(\upsilon|X)$ on $\mathcal{D}_{rollout}$ $\mathcal{D}_{rollout} \leftarrow \emptyset$
        end if
    end for
end for
for m=1:M **do**
    Sample a simulator $\hat{\rho} \sim P(\rho)$.
    Collect set of trajectories $\mathcal{D} = \{\mathcal{T}\}$ in $\hat{\rho}$ by running adaptive policy $\pi_{\theta_m}(a_{t-1}|s_t, z_t)$ with extractor $z_t = \phi_{\varphi_m}(z_{t-1}, s_t, a_{t-1}, \upsilon_t)$, where υ_t comes from q_κ.
end for

E EXPERIMENTAL DETAILS IN REAL-WORLD RIDE-HAILING PLATFORM

We collect offline data from the platform and construct our real-world simulators by imitation from data Shang et al. (2019). The results show that the order completion in the reconstructed simulators is generally consistent with the real-world data.

We train the SA-DAE in the training set and test the reconstructed data distribution in the unseen environment. The training dataset $\mathcal{D}_X$ comes from human expert data in the training set. $q_\kappa\left(\upsilon|s^{(i)}, a^{(i)}\right)$ is a neural network which outputs the Gaussian distribution parameters of υ. The dimension of the vector υ is 200 in this environment. $p_\theta\left(\psi_a|\upsilon, s^{(i)}\right)$ and $p_\theta\left(\psi_s|\upsilon\right)$ are modeled with neural networks, which output the parameters of the distributions. The action reconstruction is modeled with Gaussian distribution since it is continuous in the environment. However, the state space includes continuous and discrete features. For simplification, we assume the continuous features are independent of

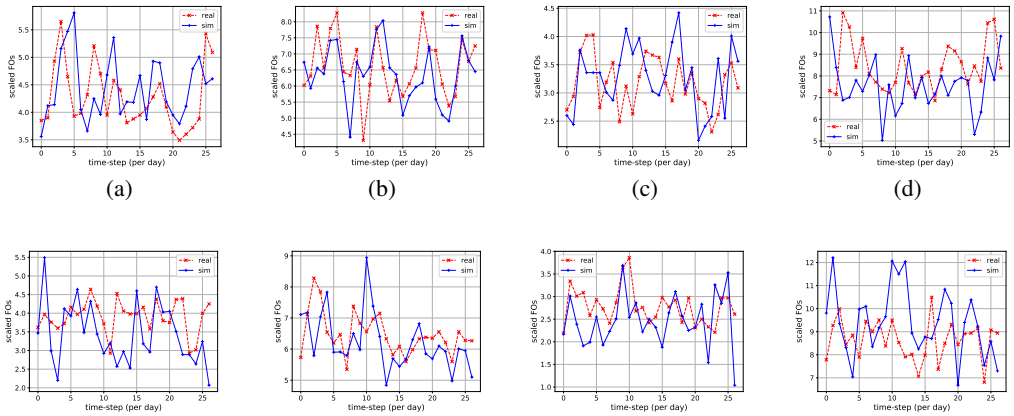

(a) (b) (c) (d)

(e) (f) (g) (h)

Figure 11: Illustration of the daily finished-order curves of the constructed simulator and real data. Each column shows the results of the same city. Each row shows the results in the same period.

discrete features. Thus we model them with Multivariate Gaussian distribution and categorical distribution respectively. The prior of υ is set to standard normal distribution, i.e., $p(\upsilon) = \mathcal{N}(0, 1)$.

We use KLD to measure the reconstruction performance. Since the dimension of state-action space is high and the distribution is complex, we use Kernel Density Estimation (KDE) Rosenblatt (1956) to estimate the probability density function (PDF) of real and reconstructed data. Then the KLD of two datasets is computed based on it. In particular,

$$KLD(\mathcal{D}_a, \mathcal{D}_b) = \frac{1}{||\mathcal{D}_a||} \sum_{x \in \mathcal{D}_a} \log \frac{f_a(x)}{f_b(x)}, \tag{13}$$

where $||\mathcal{D}_a||$ denotes the number of samples in the dataset, and f_a and f_b denote the PDF of real and reconstructed data estimated by KDE. We test the KLD every 100 epochs. Figure 12(a) shows that the KLD between the real data X and the reconstructed distribution $p_\theta(X|\upsilon)$ steadily converges to 0.6, which demonstrates nontrivial reconstruction performance. Figure 14 shows histograms for examples of real and reconstructed data on a single feature, which are also significantly correlated.

To evaluate the embedding performance of SA-DAE, we performed the hidden state prediction experiments Akkaya et al. (2019). If the embedding variables store useful information about the distribution, for a simple neural network, the KLD prediction error between arbitrary two datasets would be negatively correlated with the training epochs. We use another one-layer neural network to predict the KLD of two data pairs (X_i, X_j), given their embedding variable (υ_i, υ_j). The neural network has one 32-unit hidden layer with tanh as the activation function and links to a linear layer to predict the KLD computed by Equation 13. The neural network is initialized and retrained for the same epochs, every 100 iterations of SA-DAE learning. Figure 12(b) shows the mean absolute error (MAE). The MAE has 26% improvement than the initial variable, which implies the embedding variable is helpful to infer the relation of two distributions.

F Additional Details for OapRS

The network structure of OapRS is shown in Figure 13. In the implementation, we use two independent network structures for the value function and policy learning. Moreover, there is a skip-connection for the environment-aware layer to reuse the original input features. The embedding layer and environment-aware layer are modeled with Multilayer Perceptron (MLP). The environment-context extractor layer is modeled with a single-layer LSTM network Hochreiter & Schmidhuber (1997). We use the same network structure and hyperparameters in the two experiments, but the complexity of neural networks are different. Table 1 reports the detailed settings.

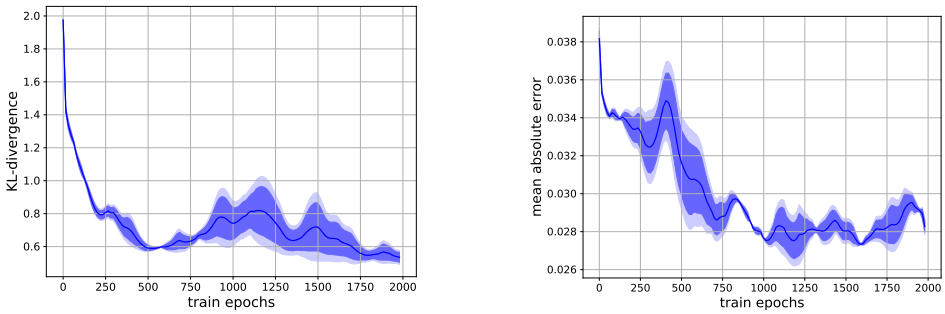

(a) KL divergence (b) mean absolute error

Figure 12: Illustration of the reconstructed and embedding performance on SA-DAE. The solid curves are the mean reward of two seeds. The dark shadow is the standard error, and the light one is the min-max range of two seeds.

In the DPR environment, we model the distribution of continuous states with Multivariate Gaussian distribution. The covariance of the Multivariate gaussian distribution should be a symmetric positive semi-definite matrix. We construct the covariance matrix based on Cholesky decomposition Golub & Van Loan (1996). In particular, a symmetric positive-definite matrix Σ is a decomposition of the form:

$$\Sigma = LL^\top,$$

where L is a lower triangular matrix with real and positive diagonal entries, and $L^\top$ denotes the transpose of L. We use a neural network with the softplus activation function to output the elements of L, where the softplus is used to output a positive value. Then, we regard the matrix $LL^\top$ as the covariance of the Multivariate Gaussian distribution. The hyperparameters of SA-DAE in the two experiments are shown in Table 2.

In addition, we use several tricks in the training process of the environment-context extractor and adaptive policy:

Larger entropy coefficient We set the entropy coefficient to 0.02 for the LSTM-based policy and 1e-5 for MLP-based policy in the two problems. We found that the smaller entropy coefficient leads to performance collapse after some iterations when training with LSTM-based policy.

Multiple environments sampling We sample from all training environments uniformly for $\nabla J(\theta)$ computation every iteration. The policy updates would be unstable and inefficient if just sampling from a single environment.

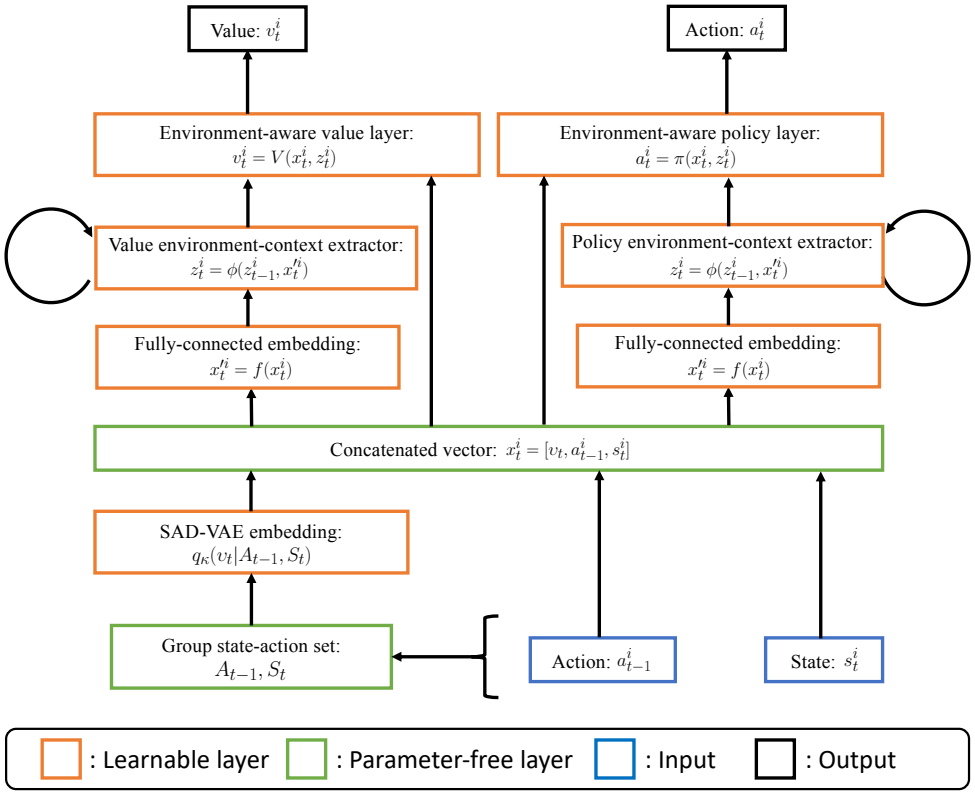

Figure 13: Illustration of the network structure for OapRS.

Table 1: The hyper-parameters of OapRS for policy learning.

Hyperparameter	LTS	DPR
Discount factor γ	0.99	0.9
Horizon H	140	30
Entropy regularization coefficient	0.02	o.oo1
PPO clipping parameter ϵ	0.2	
Learning rate	from 1e-4 to 1e-6	
Batch size	30000	120000
Sample reuse	3	
Optimizer	Adam	
L2 regularization weight	1e-6	
Activation function of hidden layer	leaky relu	
Activation function of policy output	tanh	
Fully-connected embedding f	[128, 128, 128,32]	[512, 512, 256]
Unit of environment-context extractor ϕ	64	256
Environment-aware layer of V and π	[128, 64]	[512, 256]

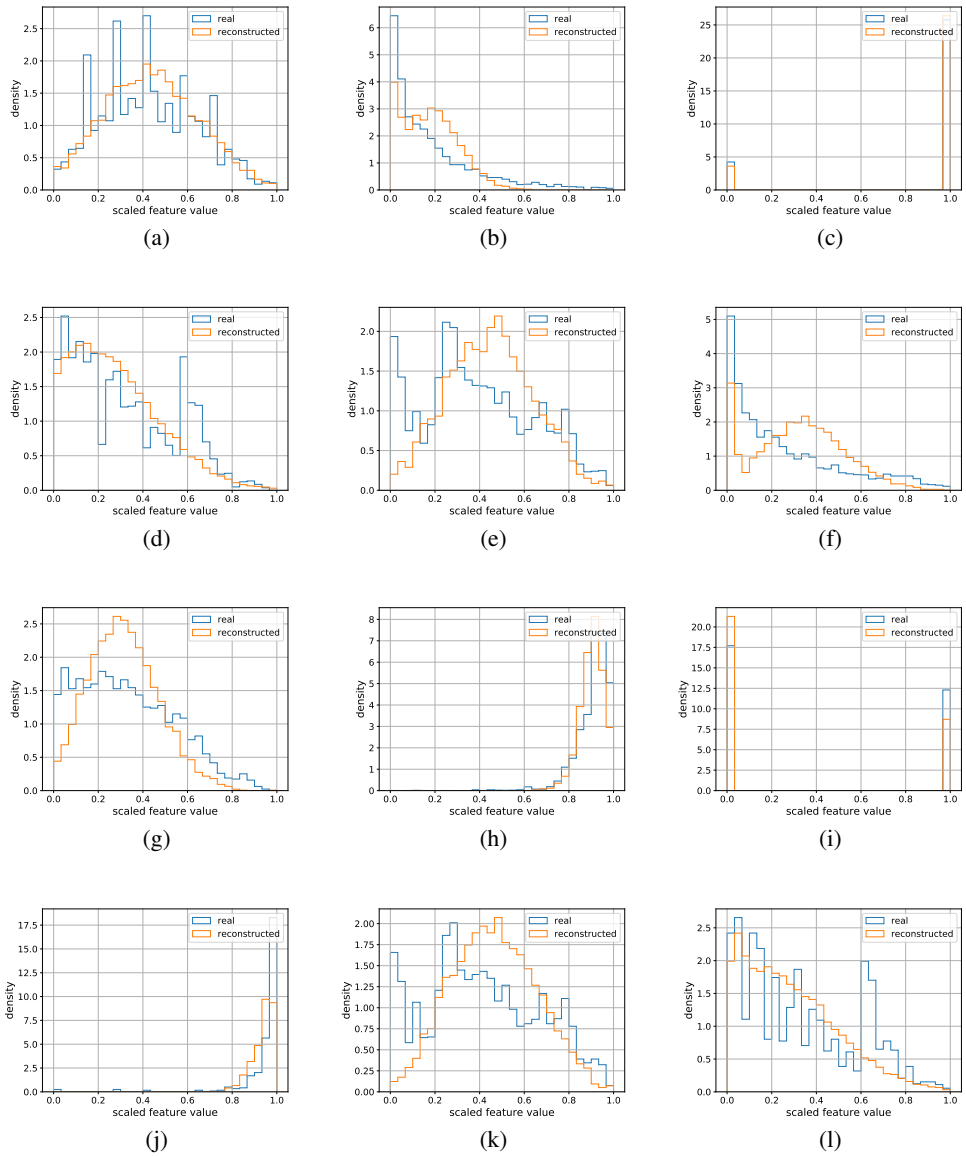

Figure 14: Illustration of the histogram about customer features of reconstructed and real data.

Table 2: The hyper-parameters of OapRS for SA-DAE.

Hyperparameter	LTS	DPR
Learning rate:	2e-5	1e-6
Layer Normalization:	False	
Optimizer:	Adam	
L2 regularization weight	0.1	0.001
activation function of hidden layer	leaky relu	
Embedding layer $q_\kappa(\upsilon\|s,a)$	[512, 512]	
Reconstructed layer $p_\theta(\psi\|\upsilon)$	[512, 512]	
units of latent code	5	200

Table 3: The averaged scaled daily rewards of real-world deployment in RDP environments

	OapRS	MOPO
before	0.9019	0.8857
after	0.9641	0.8865
improvement (%)	6.9%	0.1%